Heliyon 10 (2024) e23350

Contents lists available at ScienceDirect

Heliyon

journal homepage: www.cell.com/heliyon

# Biomass fly ash as nanofiller to improve the dielectric properties of low-density polyethylene for possible high-voltage applications

Atizaz Hussain Akram [a], Nida Naeem [a], Asif Hussain Khoja [a,*], Faisal Shahzad [b], Abraiz Khattak [a], Muhammad Iftikhar [b,c], Kashif Imran [a], Abdulaziz Al-Anazi [d], Israf Ud Din [e], Syed Sheraz Daood [f,**]

[a] U.S.-Pakistan Centre for Advanced Studies in Energy (USPCAS-E), National University of Sciences & Technology (NUST), Sector H-12 Islamabad (44000), Pakistan
[b] Department of Metallurgy and Materials Engineering, Pakistan Institute of Engineering and Applied Sciences (PIEAS), Islamabad 45650, Pakistan
[c] Department of Physics and Applied Mathematics, Pakistan Institute of Engineering and Applied Sciences, Nilore, Islamabad, 45650, Pakistan
[d] Department of Chemical Engineering, College of Engineering, King Saud University, P. O. Box 800, Riyadh 11421, Saudi Arabia
[e] Chemistry Department, College of Science and Humanities, Prince Sattam Bin Abdulaziz University, P.O. Box 173, Alkharj, 11942, Saudi Arabia
[f] Institute of Energy and Environmental Engineering, Faculty of Electrical, Energy and Environmental Engineering, University of the Punjab, Lahore 54590, Pakistan

ARTICLE INFO

*Keywords:*
Low-density polyethylene
Nanofillers
Biomass fly ash
Dielectric constant
Composites

ABSTRACT

Flexible capacitive energy storage applications require polymer nanocomposites with high dielectric properties, which can be accomplished by addition of inorganic nanofillers to the polymer matrix. Low-density polyethylene (LDPE), known for its good dielectric characteristics and wide use in electrical insulation have been investigated for the desired applications. However, the improvement of its breakdown strength still continues with the use of various nanomaterials employed as nanofillers. In this study, a waste-derived material known as biomass fly ash (BFA) as a nanofiller to improve the dielectric properties of LDPE has been explored. BFA exhibits versatility in its composition with various metal oxides, making it an attractive choice as a nanofiller. The BFA-LDPE sheets were prepared using a conventional solvent mixing and subsequent hot-pressing process, incorporating BFA loadings ranging from 1 % to 4 wt%. The effects of different BFA loadings were carefully examined, and the synthesized nanocomposites were extensively characterized using various characterization methods, such as XRD, SEM, FTIR, TGA and dielectric constant measurements, to investigate the crystallographic properties, morphology, chemical composition, and thermal stability. Among all the nanocomposites, 4 wt%BFA-LDPE exhibited the highest dielectric constant, with a value of 11.58, compared to simple LDPE that had a dielectric constant of 8.33. This improvement is ascribed to the synergistic effects of different inorganic metal oxides ($SiO_2$, MgO, and $Fe_2O_3$) present in BFA. The results showed a significant enhancement in dielectric properties, indicating that the waste-derived BFA can be purposefully applied as an effective nanofiller in the LDPE-based composites with even less than 4% loading for electrical insulating applications in future studies.

* Corresponding author.
** Corresponding author.
*E-mail addresses:* asif@uspcase.nust.edu.pk (A.H. Khoja), sdaood.icet@pu.edu.pk (S.S. Daood).

https://doi.org/10.1016/j.heliyon.2023.e23350
Received 18 May 2023; Received in revised form 29 November 2023; Accepted 1 December 2023
Available online 6 December 2023

## 1. Introduction

The polymers are insulating materials used in electrical insulation in a variety of electrical applications due to their desirable properties and low cost [1–3]. The frequent used polymers in cable insulation and accessories is polyethylene (PE) due to its high toughness and flexibility at low temperatures, minimal moisture absorption, excellent resistance, acids, alkaline compounds and solvents, as well as its potential for recycling [4]. PE is classified into several types and commercial grades, making it appropriate for a widespread range of insulation applications, both indoors and outdoors. The primary criteria for its classification are density values and the degree of branching in the chain, namely low-density polyethylene (LDPE), linear LDPE, medium-density polyethylene (MDPE) and high-density polyethylene (HDPE) [5]. The LDPE has various applications and is used in different fields including pipes, fittings, machine parts, packaging bags, containers etc. [6]. However, due to its excellent mechanical and dielectric properties with large molecular weight, and hydrophobic nature, it is often the preferred choice for power cable insulation. Additionally, its halogen free and non-polar chemical nature makes LDPE a substantially more environmentally friendly option for cable insulation compared to the conventional polyvinyl chloride (PVC)-based products. Nevertheless, when exposed to various operating and environmental conditions, LDPE suffers significant and irreversible structural degradation. These structural alterations significantly reduces its physical properties and performance [7].

Since the 1990s, investigations on polymer nanocomposites and their sub-category nanodielectrics have increased significantly [8]. These rapidly developing research outputs are not only limited to LDPE. Ferroelectric polymer-based nanocomposites and non-ferroelectric linear dielectric poly (methyl methacrylate) materials are also being used for various high-discharge applications and insulations in electrical equipment [9,10]. Typically, polymer nanocomposites are described as the polymers having uniformly dispersed nanometric-sized fillers (nanofillers) that make up less than 10 % of the total weight of the polymer [11]. Higher material performance in terms of mechanical and thermal properties were shown when nanofillers are added to a polymeric matrix [12]. Furthermore, it has been demonstrated that when there is a favourable interaction, sub-micron particles uniformly dispersed in the polymer matrix can also enhance electrical properties [13] and contribute to the materials' excellent resistance to deterioration and thermo-mechanical efficiency [14]. In contrast to typical micro composites, the utilization of nanocomposites as dielectrics has improved breakdown performance and the dielectric constant [15]. These developments are crucial for studying superior insulating materials proficient of withstanding higher voltage levels and voltage shocks, addressing the growing demands for electricity and power reliability [16].

The dielectric constant of PE with various nanofillers, such as alumina ($Al_2O_3$), silica ($SiO_2$) [17], iron oxide ($Fe_2O_3$) [18], titania ($TiO_2$) [19], zirconia (ZrO) [20] and magnesia (MgO) [21], have been the subject of numerous experimental studies up to this point. These studies have reported improved dielectric constant, subsequently enhancing the breakdown strength of the material in high voltage applications [22,23]. Additionally, it has been discovered that the dielectric constant is influenced by the interphase between the LDPE and the nanofiller, which can function as an electron trap and boost the charge storage capabilities of the material. The dielectric constant also relies on the homogenous distribution and low concentration of nanofillers [24]. However, the application of nanocomposites to enhance the dielectric constant and breakdown properties of materials is a complex topic, and it has been reported that the dielectric constant of nanocomposites is sometimes lower than that of their unfilled counterparts. For example, in the case of PE incorporating an $Al_2O_3$ nanofiller, this value was lower than that of the unfilled PE [17]. Similarly, Azmi et al. [25] prepared $MgAl_2O_4$-PP(Polypropylene) composites with increased dielectric constant than $CaCO_3$-PP nanocomposite. $MgAl_2O_4$ itself has a higher dielectric constant compared to PP, whereas $CaCO_3$ has a low dielectric constant due to enhanced polymer-nanoparticle interactions and hindered movement of entangled polymer chains. Therefore, the research has shifted from single metal oxides to multi metal oxides because of their compact structure and diverse chemical, electrical, and mechanical properties [25]. $Al_2O_3$–$SiO_2$-LDPE revealed enhancing properties compared to single metal oxides, with their high surface-to-volume ratio contributing to improved dielectric properties [26]. Clinard et al. [27] worked on $MgAl_2O_4$ nanofillers and suggested their improved mechanical strength and stability at high temperatures compared to MgO and $Al_2O_3$ due to strong ionic interactions between the metal cations and oxygen anions. Various readily available fillers in the market have been used to modify the base polymer's characteristics; however, these fillers are expensive relative to the polymer material, since they are often prepared via synthetic and complex routes. Recently, waste derived and low cost nanofillers have gained attention in this research area [24]. However, the effect of waste-derived nanofillers on the physicochemical properties of nanocomposites has yet to be thoroughly investigated.

Therefore, the aim of this work is to utilize waste derived nanofillers to enhance the dielectric properties of LDPE. A waste material of biomass-fired power plants known as biomass fly ash (BFA) include several metal oxides, including CaO, $Fe_2O_3$, MgO, $Al_2O_3$, and $SiO_2$ [28]. BFA is a fine nanopowder with a versatile chemical composition that makes it an attractive nanofiller [29][30]. It has the ability to disperse more effectively in LDPE and enhance the dielectric properties of LDPE loaded with BFA (BFA-LDPE). The dispersed nanoparticles of BFA in a LDPE matrix can attract small, charge-carrying molecules such as ions and polar molecules, potentially resulting in an overall increase in the dielectric constant [31]. Free electrons and holes can be trapped in deep traps close to the surface of BFA due to its polar and porous nature while charge carriers can aggregate at the nanofiller's surface, resulting in fewer space charges [32,33]. Thus, the synergistic effect of different metal oxides as nanofillers has the potential to significantly increase the dielectric constant of nanofiller loaded LDPE.

In this study, the BFA nanofiller is prepared and loaded on the LDPE. The characterization techniques including X-ray diffraction (XRD), scanning electron microscopy (SEM), Fourier transform infrared spectroscopy (FTIR), and thermogravimetric analysis (TGA) were utilized to analyse the morphology, structure, and thermal stability of BFA, LDPE and BFA-LDPE. Furthermore, the dielectric constant of LDPE, and BFA-LDPE is thoroughly investigated to assess the impact of BFA on the dielectric properties of BFA-LDPE in power applications.

## 2. Methods and materials

### 2.1. Preparation of BFA

In the world, various industrial sectors, including pulp, paper, textile, sugar and independent energy suppliers utilize local biomass to fuel dedicated power plants. This practice results in generation of substantial quantities of biomass fly ash. Depending on the type of fuel, boiler and operating conditions, raw samples of BFA contain varying compositions of wheat straw, rice straw, wooden packaging, and black liquor [28]. Prior to the utilization of BFA, it was dried, ground, and sieved to acquire the required particle size (0.2 mm). The sample was then washed and further purified by deionized (DI) water and ethanol. The filtrate was subsequently dried at 110 °C overnight, resulting in a powder that was further ground and calcined for 5 h at 800 °C to remove volatile components and inbound moisture at high temperatures (Fig. 1).

### 2.2. Preparation of nanofiller-LDPE

Low-density polyethylene (LDPE, NTF 0343 P, Malaysia), Xylene (98.5 %, reagent grade, Sigma-Aldrich), and BFA were the starting materials in the preparation of nano-filled LDPE composites as presented in Fig. 1. The BFA-LDPE sheets were prepared using a typical solvent mixing and subsequent hot-pressing technique. First, 5.0 g of LDPE was dissolved in 95 mL Xylene at 90 °C with constant stirring in a 200 mL beaker. Then pre-weighted BFA was added to this solution during constant stirring. The solution was evaporated during the processing, and a viscous kind of polymeric composite gel was obtained. The polymer composites were formed in different nanofiller loadings of 1, 2, 3, and 4wt% BFA. The semi-solid polymeric composite gel was transported to 6 cm × 8 cm metallic moulds. The moulds were covered with polytetrafluoroethylene (PTFE) sheets and subjected to hot pressing (Labo press, Toyo Seiki Seisakusho Ltd, Japan) at 160 °C for 5 min. The polymeric composite films were cooled to room temperature under the applied load on a hot-press. Finally, the composite films of a thickness of 1 mm were obtained. The pristine LDPE sheet was formed by a similar process without adding nanofiller as a base case to compare with BFA-LDPE.

### 2.3. Material characterization

Synthesized composites are thoroughly investigated and characterized by using different characterization techniques. XRD analysis was performed on Bruker, D8 advanced, equipped with a 25 kV power supply and a Cu Kα radiation source (λ = 1.5418 Å) fitted with 25 kV power. The data was analyzed and gathered using a step-scan of 0.02° in the range of 2θ = 10–80°. The morphological analysis of prepared samples was conducted using SEM at different magnifications with the use of JSM-6490A from JEOL Japan. This SEM offers a resolution power of 3 nm at 30 kV and variable magnification range (10–200,000X).

Using the Cary 630 (Agilent Technologies, USA) at wavenumber ranges between 4000 and 650 $cm^{-1}$, FTIR was employed for the screening of specific functional groups of synthesized materials. The existence of peaks at various wavenumbers in the FTIR spectrum

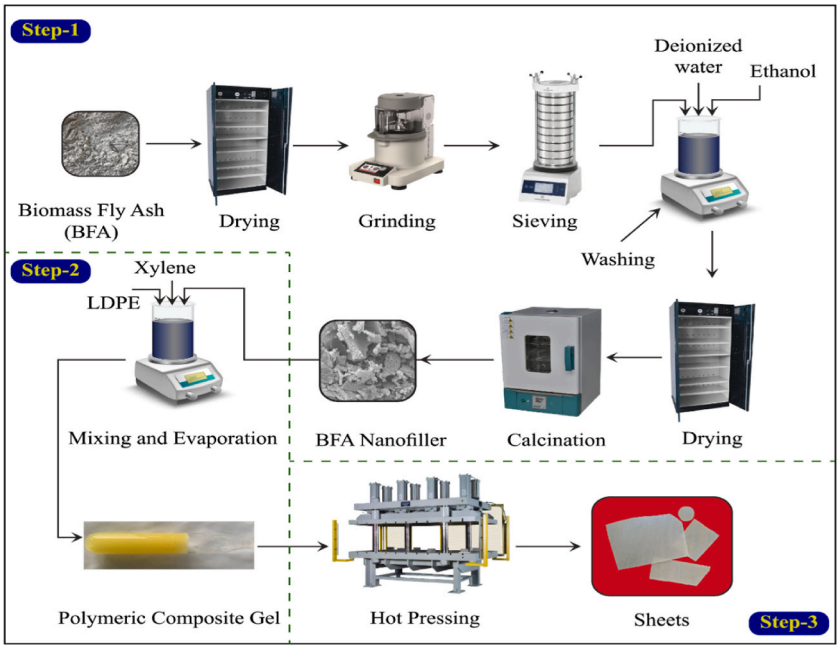


**Fig. 1.** Preparation of BFA nanofiller and BFA-LDPE nanocomposite.

can be used to assess the chemical nature and the type of bonding. By maintaining $N_2$ flow of 40 mL/min and a heating ramp of 20 °C/min at various temperature ranges up to 900 °C, the thermal stability of the materials was examined using a TGA analyzer 5500 (Discovery, series) from TA instruments, (USA).

### 2.4. Measurement of dielectric properties

At room temperature and within the frequency range of 1–150 kHz, the dielectric measurements (capacitance and dielectric loss factor) using a Gwinstek Precision LCR Meter model LCR 8110 G were performed. Prior to the measurements, the samples were coated with air dried silver to establish contacts on their surfaces. The dielectric constant ($\kappa$) is defined as the ratio of the permittivity of a material ($\varepsilon_m$) to that of free space ($\varepsilon_o$), as shown in Eq. (1):

$$\kappa = \varepsilon_\gamma = \frac{\varepsilon_m}{\varepsilon_o} \tag{1}$$

The formula in Eq. (2) is used to compute the parallel capacitor capacitance

$$C = \frac{A\varepsilon}{d} \tag{2}$$

*Where,* $A$ = area of plates, $\mathcal{E}$ = permittivity of the material and $d$ = distance between the plates.

## 3. Results and discussion

### 3.1. Physicochemical properties

The XRD spectra of LDPE, BFA, and 4% BFA-LDPE are presented in Fig. 2. Two distinct peaks are noticeable in the spectrum of LDPE at $2\theta = 21.5°$ and 23.75° (PDF# 11–0834) with the indices values of (110) and (200) show that the LDPE is in a semi-crystalline phase (degree of crystallinity 38 %) as shown in Fig. 2(a) [34]. A low-intensity peak is also visible at around $2\theta = 44°$ in Fig. 2(a), which provide insights into the degree of crystallinity in LDPE or possibly indicates the presence of HDPE impurities indicative of a characteristic low intensity peak at the same degree. Furthermore, small peak at 44° can inferred to the diffraction peaks of orthorhombic LDPE [35]. The similar peak has been reported during the Rietveld refinement of XRD spectra of LDPE when enlarged between $2\theta =$

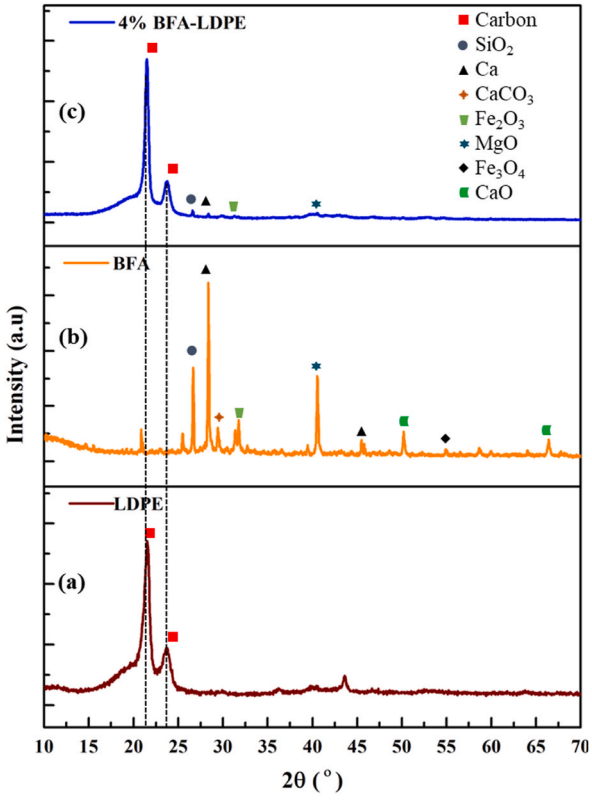


**Fig. 2.** XRD pattern of **(a)** LDPE, **(b)** BFA and **(c)** 4% BFA-LDPE.

28° and 2θ = 60° [35]. The semi quantitative level of accuracy and the analysis of the data presented in Fig. 2(a) is analogous to the other studies [35,36]. Similarly, the intensity and position of the peak can be affected by changes in the crystalline structure of LDPE or its interaction with other substances resulting from doping or impregnation therefore it disappeared after the addition of nanofiller in LDPE (Fig. 2(c)) [36–38]. BFA depicted various diffraction peaks in the crystalline phase as presented in Fig. 2(b), which corresponds to different metal oxides. The detailed XRD analysis of BFA is reported elsewhere [30]. In brief, the $SiO_2$ and $Fe_2O_3$ peaks appeared at 2θ = 26.5° (PDF# 46–1045) and 32.8° (PDF# 10–0653) with index values of (101) and (420) respectively [30]. While 2θ = 28.2° and 44° are ascribed to Ca (110) [30]. Furthermore, MgO [39], $Fe_3O_4$, and CaO [40] are also present at their respective 2θ values, as given in Fig. 2(b–c). Several distinctive diffraction peaks, which correspond to the diffractions of BFA in the 4% BFA-LDPE, appeared at their respective *hkl* indices as shown in Fig. 2(c). By comparing the distinctive peaks of the BFA-LDPE with the standard diffraction peaks of LDPE and BFA, it was proved that the crystal planes in the composite are consistent and compatible with the crystal planes of the typical diffraction peaks of BFA and LDPE. This comparison also demonstrates that the addition of BFA does not significantly alter the crystallography of LDPE. Moreover, no additional heterogeneous materials were formed after the hot-pressing of the BFA and LDPE [41]. The analysis of the data presented in Fig. 2 also reports that crystallographic evaluations of LDPE and BFA are comparable with the peaks observed in 4% BFA-LDPE.

SEM was carried out to evaluate the surface changes in the materials. The micrographs of pure LDPE at various magnifications are shown in Fig. 3(a–b). It can be seen that the pure LDPE possesses a smooth surface with no discernible defects, though small pieces on its surface may be impurities. The smooth and homogeneous surface of LDPE leads us to believe that the LDPE crystal phase cannot be detected at these magnifications [42]. By comparing LDPE with 4% BFA-LDPE, no apparent of agglomeration in the cross section of the 4% BFA-LDPE was observed Fig. 3(c–d) [41]. These results indicate that BFA is dispersed within the polymer matrix. SEM analysis was also performed on samples loaded with BFA, with a focus on those exhibiting the best dielectric properties, as demonstrated by 4% BFA-LDPE during initial testing.

The FTIR analysis of LDPE and 4% BFA-LDPE in the range of 600–4000 $cm^{-1}$ is presented in Fig. 4. LDPE consisting of $–CH_2$ groups exhibits characteristic absorption bands in the range of 720 $cm^{-1}$ to 2926 $cm^{-1}$. The $CH_2$ asymmetric and symmetric stretches are represented by the peaks at 2917 $cm^{-1}$ and 2852 $cm^{-1}$, respectively, while the peaks at 1465 $cm^{-1}$ and 721 $cm^{-1}$ correspond to the deformation vibration band and in-plane rocking vibration band of $–CH_2$, respectively [43]. A significant LDPE peak at 1377 $cm^{-1}$, the $–CH_3$ umbrella mode, differentiates LDPE from HDPE. This peak is attributed to short alkyl side chains having the structural formula of $–(CH_2)_5–CH_3$ in LDPE; which pushes the polymer chains apart, resulting in a reduction in material density. The spectrum of LDPE shows the prominent umbrella mode peak at 1377 $cm^{-1}$ attributed to the $–CH_3$ groups in the side chains [44,45] as shown in Fig. 4(a).

In 4% BFA-LDPE, weak bands corresponding to major oxides (-*Si*-O and CaO) present in BFA appear in the region of 724 $cm^{-1}$ to 1100 $cm^{-1}$ (Fig. 4(b)) [28]. The -*Si*-O is detected at 1100 $cm^{-1}$, while the peaks in the range of around 724 $cm^{-1}$ to 924 $cm^{-1}$ indicate the presence of CaO [30,46]. It is worth noting that peaks at 1712 $cm^{-1}$ and 3230 $cm^{-1}$ are also observed, corresponding to the carbonyl (-C═O) [47] and -*O*-H bond stretching [48] as presented in Fig. 4(c).

The emergence of newly developed functional (O–H and C═O) groups, as well as modifications to already existing groups and

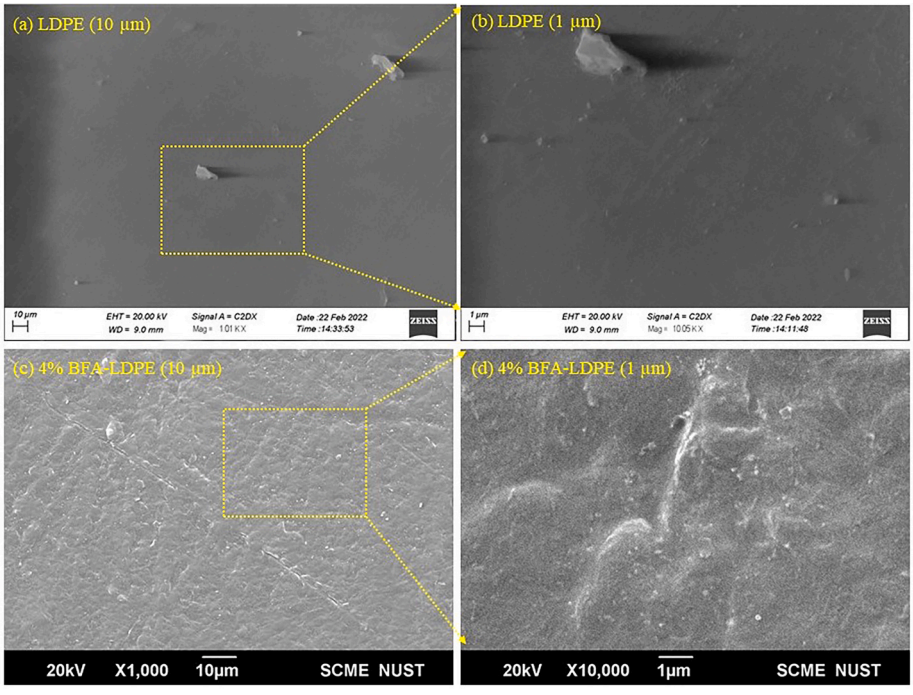


**Fig. 3.** SEM micrographs of **(a-b)** LDPE **(c-d)** 4% BFA-LDPE.

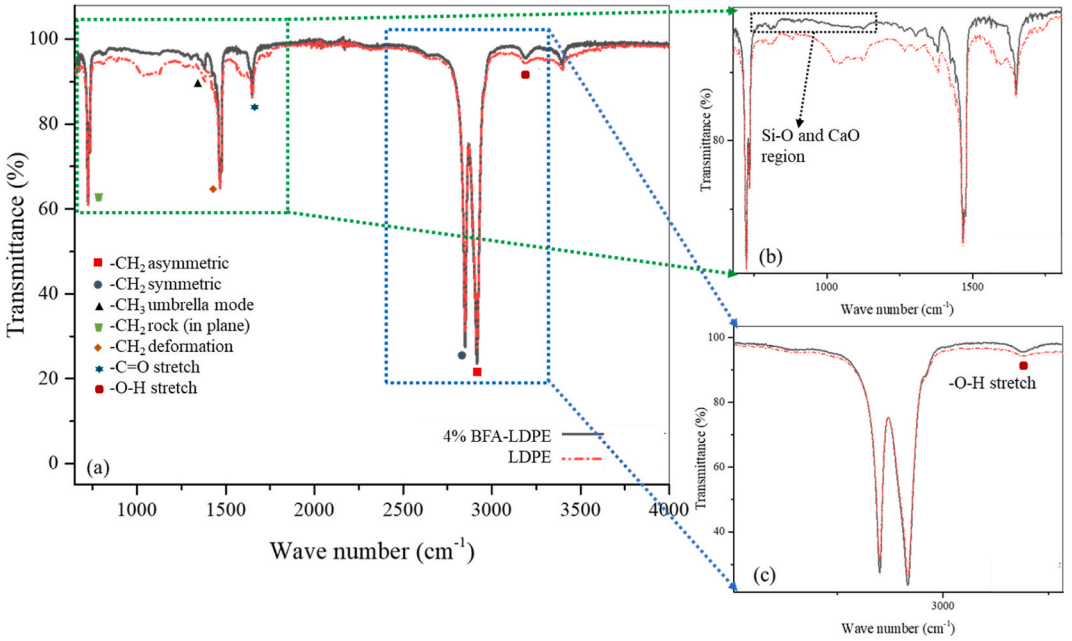


**Fig. 4.** **(a)** FTIR spectra of LDPE and 4% BFA-LDPE **(b)** enlarge metal oxide and C═O region and **(c)** enlarged C–H and O–H region.

chemical changes, leads to slight shifts and broadening of absorption bands in the FTIR spectrum. Additionally, these changes can introduce structural defects such as vacancies and the formation of new phases due to oxidation processes. These defects have a substantial impact on the dielectric properties of 4% BFA-LDPE [47,49] because the structural defects play a key role in altering breakdown strength, charge mobility, and sensitivity to temperature [50]. The analysis of the FTIR spectra presented in Fig. 4 of LDPE and the overall characteristics of BFA are representative of the spectra observed for the 4% BFA-LDPE.

The thermograms of pure LDPE and BFA-LDPE with changing wt% of BFA are given in Fig. 5. All the polymer samples start to degrade at 350 °C and remain stable below 500 °C, as shown in Fig. 5(a). Pure LDPE begins to decompose at a relatively low temperature, approximately 475 °C. In contrast, 4 % nanofiller LDPE begins to break down at 500 °C, indicating improved stability in BFA-LDPE samples as the wt% of BFA increases (Fig. 5(b)). However, it's important to note that excessive BFA content may lead to a decline in the composite material's insulating capabilities.

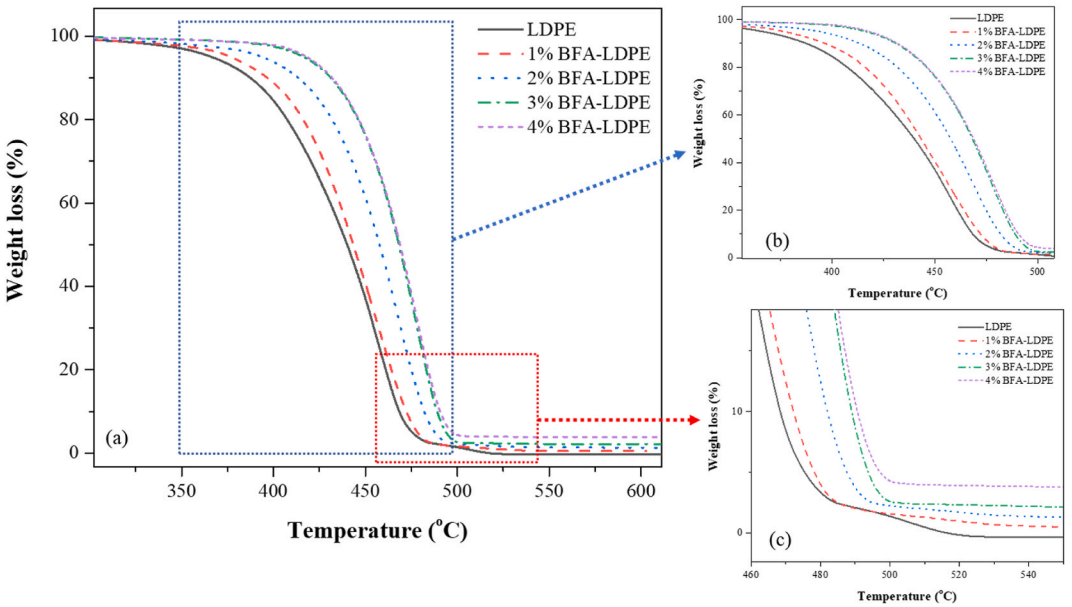


**Fig. 5.** **(a)** TGA of prepared samples LDPE and 1-4% BFA - LDPE **(b)** enlarged degradation stage **(c)** enlarged passive stage.

It can be inferred from the literature that the increase in thermal conductivity caused by the addition of BFA to LDPE is closely related to the formation of thermally conductive networks. These networks result from the presence of highly conductive inorganic particles within 1-4% BFA-LDPE, a consequence of BFA incorporation [51,52]. Furthermore, LDPE polymer typically undergo thermal breakdown, which causes the generation of free radicals at weak bonds, often at chain ends. This process is followed by a series of main free radical chain transfer reactions that continue until the entire matrix is affected. The motion restriction introduced by BFA in LDPE helps prevent these chain transfer reactions, ultimately enhancing the thermal stability of the nanocomposites due to BFA's diverse physiochemical properties [53]. Thus, BFA addition hinders the degradation of LDPE and increases the thermal parameter of the composite. An additional peak is observed between 500 and 550 °C (Fig. 5(c)) which can be attributed to the oxidation reaction, consistent with the findings from FTIR studies.

### *3.2. Dielectric constant analysis*

The relationship between pure LDPE and BFA-LDPE composites with varying loading concentrations, in terms of dielectric constant and frequency at room temperature (25 °C), is given in Fig. 6. It is evident that the dielectric constant of BFA-LDPE is larger than that of the pure LDPE, and it increases with an increase in filler content when the frequency is constant (1 kHz). As shown in Fig. 6(a), pure LDPE has the value of dielectric constant equal to 8.33, while it is increased linearly from 8.70 to 11.58 with BFA loading from 1 to 4%. Specifically, 1% BFA-LDPE, 2% BFA-LDPE, 3% BFA-LDPE, and 4% BFA-LDPE have dielectric constant values of 8.70, 9.68, 11.21, and 11.58, respectively. Thus, the 4% BFA-LDPE displays the maximum dielectric constant due to the higher concentration of BFA which enhances the physiochemical properties of 4% BFA-LDPE.

The presence of various oxides in BFA contributes to the increase in dielectric constant. The XRD pattern shows the presence of $SiO_2$, MgO, and $Fe_3O_4$ in BFA-LDPE composite, which influences the dielectric constant and demonstrates a synergetic effect. The presence of $SiO_2$ increases the number of dipoles and intensifies the interfacial polarization due to the increase of certain molecule fragments, dipolar species, and ions [17]. MgO has a dielectric constant greater than LDPE, exhibits better molecular motion that assists the movement of carriers along with better oriented dipoles, further increasing the dielectric constant of the composite [21]. On the other hand, $Fe_3O_4$ forms a conductive chain in the LDPE matrix due to its magnetic properties and influences the molecular arrangement of LDPE, enhancing the dielectric constant [18]. Due to the synergistic effect of all the given metal oxides, the dielectric constant of 4% BFA-LDPE increases, making it suitable choice for further studying its dielectric behaviour with varying frequency.

Fig. 6(b) shows the dependency of 4% BFA-LDPE dielectric constant on varying frequencies, and it decreases gradually from 0 Hz to 30 kHz. After 30 kHz, it decreases sharply to 150 kHz, which shows a higher dielectric constant and the availability of free charge motion within the material. As frequency rises, there is less time for the dipoles to align before the field direction changes, which results in a drop in dielectric constant. But dipoles can align themselves more easily at lower frequencies, which results in a greater dielectric constant [54].

## 4. Conclusion

The 1-4 wt% BFA-LDPE nanocomposite sheets were prepared by using solvent mixing and hot-pressing technique, and their physiochemical properties were analyzed using various techniques. It can be evidenced from the XRD of 4% BFA-LDPE that the crystalline structure of LDPE has not been significantly changed by the addition of BFA. Furthermore, SEM analysis confirms that the BFA is well dispersed in LDPE without any significant agglomeration. The FTIR spectra revealed that major oxides contributing to the increasing dielectric constant, namely $SiO_2$, MgO, and $Fe_2O_3$, which are present in BFA. Additionally, thermal analysis (TG) provided the additional proof of improved thermal stability. In comparison to pure LDPE, the addition of BFA increased the dielectric constant of 4% BFA-LDPE by 28 %, rising from 8.33 to 11.58. This enhancement in dielectric constant is attributed to the synergistic effect of $SiO_2$, MgO and $Fe_2O_3$ present in BFA. These results demonstrate a significant improvement in the properties of LDPE when BFA is used as nanofiller. Moreover, BFA, derived from waste, offers a more cost-effective alternative to commercially available oxides. This leads to the conclusion that the BFA warrants further investigation for accurate and real time electrical applications in the future.

## CRediT authorship contribution statement

**Atizaz Hussain Akram:** Writing - original draft, Validation, Methodology, Investigation, Data curation. **Nida Naeem:** Writing - original draft, Software, Methodology, Investigation, Formal analysis, Data curation. **Asif Hussain Khoja:** Writing - review & editing, Writing - original draft, Supervision, Resources, Project administration, Conceptualization. **Faisal Shahzad:** Writing - review & editing, Validation, Investigation, Conceptualization. **Abraiz Khattak:** Methodology, Investigation, Conceptualization. **Muhammad Iftikhar:** Validation, Software, Investigation. **Kashif Imran:** Writing - review & editing, Validation, Conceptualization. **Abdulaziz Al-Anazi:** Writing - review & editing, Project administration, Funding acquisition. **Israf Ud Din:** Writing - review & editing, Software, Resources. **Syed Sheraz Daood:** Writing - review & editing, Writing - original draft, Validation, Formal analysis.

## Declaration of competing interest

The authors declare that they have no known competing financial interests or personal relationships that could have appeared to influence the work reported in this paper.

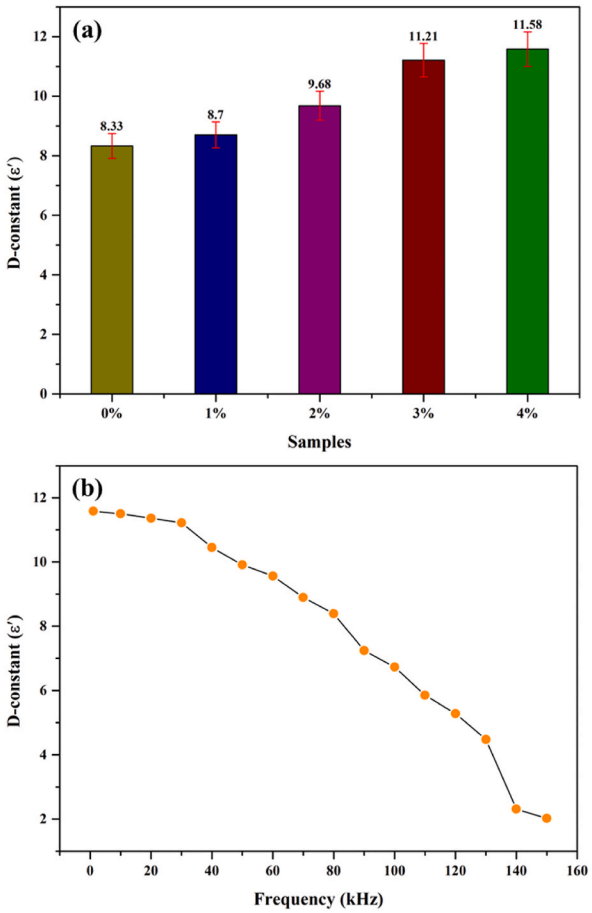


**Fig. 6.** (**a**) Dielectric constant for various loadings of BFA over LDPE and (**b**) dielectric constant of 4% BFA-LDPE with respect to frequency variations.

## Acknowledgments

The authors gratefully acknowledge the Researchers Supporting Project Number (RSPD2023R534), King Saud University, Riyadh, Saudi Arabia.

## References

[1] H. Lamnii, et al., Experimental investigation and modeling attempt on the effects of ultraviolet aging on the fatigue behavior of an LDPE semi-crystalline polymer, Int. J. Fatig. 142 (2021), 105952.
[2] F. Mebarki, E. David, Dielectric characterization of thermally aged recycled Polyethylene Terephthalate and Polyethylene Naphthalate reinforced with inorganic fillers, Polym. Eng. Sci. 58 (5) (2018) 701–712.
[3] A. Hedir, et al., Experimental and predicted XLPE cable insulation properties under UVRadiation, Turk. J. Electr. Eng. Comput. Sci. 28 (3) (2020) 1763–1775.
[4] J. Martinez-Colunga, et al., Effect of ultrasonic irradiation on low-density polyethylene molecular structure, Polym. Bull. 77 (10) (2020) 5303–5321.
[5] A.K. Rodriguez, et al., Effect of UV-aging on the mechanical and fracture behavior of low density polyethylene, Polym. Degrad. Stabil. 180 (2020), 109185.
[6] E.A. Morris, W.H. Siew, Partial discharge activity in polymeric cable insulation under high voltage AC and DC, in: 2017 52nd International Universities Power Engineering Conference (UPEC), IEEE, 2017.
[7] L.D. Gómez-Méndez, et al., Biodeterioration of plasma pretreated LDPE sheets by Pleurotus ostreatus, PLoS One 13 (9) (2018), e0203786.
[8] G.C. Montanari, et al., Modification of electrical properties and performance of EVA and PP insulation through nanostructure by organophilic silicates, IEEE Trans. Dielectr. Electr. Insul. 11 (5) (2004) 754–762.
[9] Q. Wang, et al., *$Bi_{0.5}Na_{0.5}TiO_3$-based relaxor-ferroelectric ceramics for low-electric-field dielectric energy storage via bidirectional optimization strategy*, Chem. Eng. J. 452 (2023), 139422.
[10] B. Xie, et al., High energy storage performance of PMMA nanocomposites utilizing hierarchically structured nanowires based on interface engineering, ACS Appl. Mater. Interfaces 13 (23) (2021) 27382–27391.
[11] T. Lewis, Nanometric dielectrics, IEEE Trans. Dielectr. Electr. Insul. 1 (5) (1994) 812–825.
[12] N. García, et al., Comparing the effect of nanofillers as thermal stabilizers in low density polyethylene, Polym. Degrad. Stabil. 94 (1) (2009) 39–48.
[13] F. Guastavino, et al., Processing LDPE-EVA blend with montmorillonite and silica nanoparticles, in: 2013 Annual Report Conference on Electrical Insulation and Dielectric Phenomena, IEEE, 2013.
[14] W.A. Izzati, et al., Partial discharge characteristics of polymer nanocomposite materials in electrical insulation: a review of sample preparation techniques, analysis methods, potential applications, and future trends, Sci. World J. 2014 (2014).

[15] E. Helal, et al., Evaluation of dielectric behavior of polyethylene/thermoplastic elastomer blends containing zinc oxide (ZnO) nanoparticles for high voltage insulation, in: 2016 IEEE Electrical Insulation Conference (EIC), IEEE, 2016.
[16] M.M. Alam, et al., Improved dielectric constant and breakdown strength of γ-phase dominant super toughened polyvinylidene fluoride/$TiO_2$ nanocomposite film: an excellent material for energy storage applications and piezoelectric throughput, Nanotechnology 28 (1) (2016), 015503.
[17] D. Panaitescu, et al., Effects of $SiO_2$ and $Al_2O_3$ nanofillers on polyethylene properties, J. Appl. Polym. Sci. 122 (3) (2011) 1921–1935.
[18] Q. Chi, et al., Enhanced thermal conductivity and dielectric properties of iron oxide/polyethylene nanocomposites induced by a magnetic field, Sci. Rep. 7 (1) (2017) 1–11.
[19] N.M. Abdel-Gawad, et al., Experimental measurements of partial discharge activity within LDPE/$TiO_2$ nanocomposites, in: 2017 Nineteenth International Middle East Power Systems Conference (MEPCON), IEEE, 2017.
[20] H.H. Redhwi, et al., Durability of LDPE nanocomposites with clay, silica, and zinc oxide—Part I: mechanical properties of the nanocomposite materials, J. Nanomater. 2013 (2013).
[21] K. Ishimoto, et al., Superiority of dielectric properties of LDPE/MgO nanocomposites over microcomposites, IEEE Trans. Dielectr. Electr. Insul. 16 (6) (2009) 1735–1742.
[22] K.M. Morteza Nahvi, Amirreza Mohammadpour, Mohammad mahdi Parsafar, Experimental Analysis of lean premixed natural gas-air high swirl flame chemiluminescence and flame spectrum in visible wavelengths, in: The 8th Fuel and Combustion Conference of Iran, University of Tabriz, Tabriz, Iran, 2020.
[23] F. Ciuprina, et al., Dielectric properties of LDPE-$SiO_2$ nanocomposites, in: 2010 10th IEEE International Conference on Solid Dielectrics, IEEE, 2010.
[24] A. Samad, et al., Structure and breakdown property relationship of polyethylene nanocomposites containing laboratory-synthesized alumina, magnesia and magnesium aluminate nanofillers, J. Phys. Chem. Solid. 120 (2018) 140–146.
[25] S. Dash, et al., Synthesis of $MgAl_2O_4$ spinel by thermal plasma and its synergetic structural study, J. Alloys Compd. 726 (2017) 1186–1194.
[26] N. Rubaian, A.A. Al-Arainy, Influence of adding nano particles on dissipation factor and volume resistivity of polymer, in: 2022 Muthanna International Conference on Engineering Science and Technology (MICEST), IEEE, 2022.
[27] F. Clinard Jr., G. Hurley, L. Hobbs, Neutron irradiation damage in MgO, $Al_2O_3$ and $MgAl_2O_4$ ceramics, J. Nucl. Mater. 108 (1982) 655–670.
[28] M.A. Munawar, et al., Biomass ash characterization, fusion analysis and its application in catalytic decomposition of methane, Fuel 285 (2021), 119107.
[29] A.U. Hasanat, et al., Thermocatalytic partial oxidation of methane to syngas ($H_2$, CO) production using Ni/$La_2O_3$ modified biomass fly ash supported catalyst, Results in Engineering 19 (2023), 101333.
[30] N. Naeem, et al., Partial oxidation of methane over biomass fly ash (BFA)-supported Ni/CaO catalyst for hydrogen-rich syngas production, Res. Chem. Intermed. 48 (5) (2022) 2007–2034.
[31] F. Nilsson, et al., Influence of water uptake on the electrical DC-conductivity of insulating LDPE/MgO nanocomposites, Compos. Sci. Technol. 152 (2017) 11–19.
[32] A.T. Hoang, et al., Charge transport in LDPE nanocomposites Part I—experimental approach, Polymers 8 (3) (2016) 87.
[33] E. Kubyshkina, M. Unge, B. Jonsson, Band bending at the interface in Polyethylene-MgO nanocomposite dielectric, J. Chem. Phys. 146 (2017), 051101.
[34] F. Marinkovic, et al., Methods for quantitative determination of filler weight fraction and filler dispersion degree in polymer composites: example of low-density polyethylene and NaA zeolite composite, Appl. Phys. A 125 (9) (2019) 1–9.
[35] A.A. Alsaygh, et al., Characterization of polyethylene synthesized by zirconium single site catalysts, Applied Petrochemical Research 4 (1) (2014) 79–84.
[36] H.M. Moghaddam, et al., The $TiO_2$–clay-LDPE nanocomposite packaging films: investigation on the structure and physicomechanical properties, Polym.-Plast. Technol. Eng. 53 (17) (2014) 1759–1767.
[37] W. Oliani, et al., Preparation and Characterization of Polyethylene Nanocomposites with Clay and Silver Nanoparticles, 2017, pp. 709–718.
[38] D. Tripathi, T. Dey, Thermal conductivity, coefficient of linear thermal expansion and mechanical properties of LDPE/Ni composites, Indian J. Phys. (2013), 052070.
[39] A. Almontasser, A. Parveen, A. Azam, Synthesis, characterization and antibacterial activity of magnesium oxide (MgO) nanoparticles, IOP Conf. Ser. Mater. Sci. Eng. 577 (2019), 012051.
[40] L. Zhuang, et al., Preparation and characterization of $Fe_3O_4$ particles with novel nanosheets morphology and magnetochromatic property by a modified solvothermal method, Sci. Rep. 5 (1) (2015), 9320.
[41] L. He, et al., Enhanced thermal conductivity and dielectric properties of h-BN/LDPE composites, Materials 13 (21) (2020) 4738.
[42] V.V. Panic, et al., *Composite Hydrogels Based On Poly (Methacrylic Acid) and High Concentrations Of Lta Zeolite: Basic Structural, Morphological, Swelling, Thermal, and Mechanical Properties.* Morphological, Swelling, Thermal, and Mechanical Properties, 2020.
[43] F. Doğan, et al., Conducting polymer composites based on LDPE doped with poly(aminonaphthol sulfonic acid), J. Electrost. 94 (2018) 85–93.
[44] B.J.S. Smith, The infrared spectra of polymers, Part I: introduction 36 (7) (2021) 17–22.
[45] S. Das Kumar, An approach to low density polyethylene biodegradation by Bacillus amyloloquefaciens, Journal 3 Biotech 5 (2015) 81–86.
[46] R. Mohadi, et al., Preparation calcium oxide from chicken eggshells, Sriwijaya Journal of Environment 1 (2016) 32–35.
[47] Ł. John, M. Janeta, S. Szafert, Synthesis of cubic spherosilicates for self-assembled organic–inorganic biohybrids based on functionalized methacrylates, New J. Chem. 42 (1) (2018) 39–47.
[48] S. Ramachandran, et al., IOP Conference Series: Materials Science and Engineering, vol. 310, IOP Publishing, 2018, 012139.
[49] C. Qiu, et al., Effects of oxygen-containing functional groups on carbon materials in supercapacitors: a review, Mater. Des. 230 (2023), 111952.
[50] J. Qiu, et al., Preparation and application of dielectric polymers with high permittivity and low energy loss: A mini review 139 (24) (2022), 52367.
[51] X. Huang, P. Jiang, T. Tanaka, A review of dielectric polymer composites with high thermal conductivity, IEEE Electr. Insul. Mag. 27 (4) (2011) 8–16.
[52] S. Takahashi, et al., Dielectric and thermal properties of isotactic polypropylene/hexagonal boron nitride composites for high-frequency applications, J. Alloys Compd. 615 (2014) 141–145.
[53] R. Koralege, C. Jayasuriya, Synthesis and characterization of polystyrene-clay composites, J. Emerg. Trends Eng. Appl. Sci. 6 (4) (2015) 248–252.
[54] N. Rao, et al., HVDC Cable: LDPE Nano dielectric and its response to low frequencies, in: 2018 IEEE International Conference on High Voltage Engineering and Application (ICHVE), IEEE, 2018.